Online ISSN: 2981-0396 Print ISSN: 2981-0388

International Journal of Iron & Steel Society of Iran

Journal Homepage: https://journal.issiran.com/

Research Article

Evaluation of Mechanical Properties of Welding ST-37 Steel Structures With Two Types of Welding Processes FCAW and SMAW

M. Mohammadi Soleymani *[1], E. Mehrabi Gohari *[2], A. R. Zahedian [3]

[1] *Mechanical Engineering, Payame Noor University, Tehran, Iran*
[2] *Department of Mechanical Engineering, Technical and Vocational University Tehran, Iran.*
[3] *Department of Structural Engineering, Bandar Abbas Branch, Islamic Azad University, Bandar Abbas, Iran*

ARTICLE INFO

Keywords:

FCAW, SMAW, Steel Structures, Mechanical Properties.

Article history:

Received 11 July 2024
Received in revised form 11 October 2024
Accepted 26 November 2024

ABSTRACT

ST-37 steel is applied in the construction of steel structures due to its good strength, toughness, and high weldability. In this study, two samples of ST-37 steel joint were prepared using E71T filler metal by FCAW powder coating process and E7018 electrode by SMAW method. Tensile strength, hardness, and impact resistance of the weld were examined. The results showed that the final weld strength of both welding methods was higher than 400MPa so that therefore the tensile sample from the base metal of ST-37 failed. The final strength values obtained in the FCAW welded samples were higher than in the SMAW welded samples. Hardness test results showed that the hardness of the heat-affected area increased compared to ST-37 steel in both welding methods. The mean weld metal hardness was (207) SMAW and (184) FCAW Vickers. Vickers hardness values for the base metal and the heat-affected zone also showed the same behavior as the weld metal in the two samples. The hardness average values of HAZ on both sides of the weld joint were higher than the base metal. The impact test results showed that the average impact energy of weld metal (SMAW 86J) is higher than the average impact energy of weld metal (FCAW 81J). Therefore, FCAW and Filler E71T meet the requirements of final strength and weld resistance by the seismic criteria of AISC Regulation 341-10 and also the tenth article of the National Building Regulations of Iran.

1. Introduction

Welding, as one of the techniques exercised to joint fragments, is widely employed in the industry; however, Base Metal (BM), Weld Metal (WM), and Heat-affected Zone (HAZ) have different mechanical behaviors because of the heterogeneity caused by welding [1]. Apart from the mechanical considerations related to joint design, the welding procedure, filler material, heat input, number of welding passes, etc., affect the microstructure of the weld in the joints and, in turn, affect the amount of heat-affected zone and residual stresses in the base metal [2]. Moreover, for structural steels, the strength of the welded joints determines the strength of the structure. For practical applications, welded joints are subjected to cyclic loading and fatigue in various ways; therefore,

* *Corresponding Author*
Email: mmsoleymani@pnu.ac.ir, e.mehrabi@pnu.ac.ir
Address: Mechanical Engineering, Payame Noor University (PNU), Tehran, Iran
Department of Mechanical Engineering, Technical and Vocational University Tehran, Iran
1. Assistant Professor, 2. Assistant Professor, 3. M. S.

DOI: http://10.22034/IJISSI.2024.2035314.1297
Published by ISSI (Iron & Steel Society of Iran)

welding is an essential factor in reducing the fatigue life of structural components. Welded joints assessment is a significant challenge in the industry for two reasons: first, welds tend to have weak zones in a structure due to stress concentration effects and weak material properties; second, it is challenging to predict their behavior accurately, which is partly due to the difficulty of defining the properties of the material, which are different during welding and the HAZ [3]. Many structural components in automobiles, pressure vessels, vehicles, geological equipment, spacecraft, etc., are made of welded joints. Butt welding is one of the most common weldings in the construction of structures. The widespread application of butt welding in various structures, including marine and nuclear, offers researchers the possibility of analyzing the behavior of the weld under different loading conditions [4]. However, studies have been conducted on the effect of welding input heat on the properties of high-strength steel structures. So far, insufficient research has been undertaken on welding input heat's effects on welded joints' corrosion. Low-carbon steel is one of the most critical weldable metals, attributed to several factors, such as its high weldability. Moreover, the historical abundance and demand for low-carbon steel have caused scientists and engineers to develop ways to weld. These developments include chemical compositions of fillers and power sources for welding low-carbon steel [5]. Another reason is its conductivity compared to other metals because it contains very little carbon and few other alloying elements. The drawback prevents the formation of brittle microstructures such as martensite. All this eliminates the risks of weld failures, such as hydrogen cracking. As the amount of carbon increases, the problem of welding also arises. Furthermore, it is easier to weld steel sheets with low carbon [6]. Flux Cored Arc Welding (FCAW) was first developed in the early 1950s as an alternative to Shielded Metal Arc Welding (SMAW). The advantage of FCAW over SMAW is that it is no longer necessary to use the rod electrodes used in SMAW. The advantage makes FCAW overcome the limitations of SMAW [7-8]. The FCAW technique will likely be a ubiquitous procedure using the appropriate filler metal (consumable electrode). Additionally, shielding gas is no longer needed by using electrodes, which makes this technique appropriate for outdoor welding or windy conditions. It requires less operator skill than SMAW for high-velocity applications and less primary cleaning for metals [10-9]. In a paper, Jatemoku et al. [11] studied the effect of welding current changes in SMAW and FCAW procedures of joining dissimilar materials JIS G3101 SS400 and ASTM A36 with a thickness of 10 mm. In the SMAW, however, E7018 and FCAW electrodes and welding currents of 60, 75, and 90 Amps are applied, while E71T-1 welding wire and welding current were 190, 205, and 220 Amps in the FCAW. The results indicated that the welding procedure's current affects the material's hardness and microstructure. The higher the welding current, the lower the hardness of the material, and vice versa. The highest hardness values in SMAW and FCAW are in currents of 60 and 190 amperes. Subsequently, the current in the welding procedure also affects the microstructure produced in the weld and HAZ. The formed microstructure contains pearlite and ferrite. The higher the welding current, the higher the percentage of pearlite produced and the lower the percentage of ferrite. In another study, the distortion angle, microstructure, and welding hardness of St 37 steel sheet produced by the FCAW applying welding currents of 80, 110, and 140 Amps are studied. Moreover, the CO_2 and E71T-1 welding wires are employed in a flat position. As the results show, increasing the welding current may reduce the hardness in all weld zones and cause a higher level of thermal distortion in the weld joint, particularly in the HAZ. The microstructural transformation was also observed in the welded sample using different welding currents. Both heat input and cooling rate exposed to the welded sample played a significant role in determining the properties [12]. In their paper, Jennifer et al. [13] studied the effect of welding current on corrosion rate and hardness on WM, HAZ, and BM of St37 steel. St37 steel sheets were welded with welding current variations of 75, 85, and 95 amps, and the technique applied to test the corrosion rate was ASTM G31-72 standard. Based on the weight loss and corrosion solution test, NaCl solution with a concentration of 3% is utilized; the results showed that the highest average corrosion rate was in the welded sheet with a current of 95, 85, and 75 Amps, respectively. Furthermore, testing the hardness of the material at a current of 75, 85, and 95 Amps shows that the highest hardness value occurs in the weld metal region with a lower welding current. The choice of current during the welding procedure is shown to significantly affect the corrosion rate and hardness of the welded joint (weld metal).

Since structure steel is used abundantly and welding methods FCAW and SMAW are used a lot, the comparison of the mechanical properties of these two methods has not been done on St37. Therefore, in this paper, the welding joints of ST-37 were studied by conducting several mechanical tests (including the transverse tension of the weld, hardness measurement, and impact test at room temperature and fracture profile of the fracture sections resulting from the impact test by a scanning electron microscope [SEM]) while performing FCAW and SMAW techniques.

2. Materials and Methods

ST-37 steel was chosen for this research because of its wide application in steel structures with suitable mechanical properties, weldability, and optimal toughness at low temperatures. However, an ST-37 steel sheet with dimensions of 150 x 300 and a thickness of 12 mm was utilized for welding. Table 1. presents the quantum analysis of the chemical composition of ST-37 steel obtained by the Quantometer. For FCAW, ASW E71T-1C welding wire was used with the chemical composition presented

in Table 2. Moreover, the E7018 electrode (manufactured by Ama Company) was used for SMAW welding with the chemical composition presented in Table 3.

Accordingly, FCAW and SMAW were exercised to join the sheets. However, FCAW is applied due to its widespread application for welding structures. Fig. 1. shows the schematic of the welding joints and the preparation procedure before welding. Tables 4 and 5. present the other parameters for FCAW and SMAW, respectively. Following the welding operation, radiographic and penetrative liquid tests were performed to ensure the strength of the weld at the welding joint.

Table 1. Chemical composition of ST-37 steel base metal (per weight percentage).

Fe	C	Mn	Si	P	S
Balance	0.15	0.45	0.3	0.024	0.03

Table 2. Chemical composition of ASW E71T-1C welding wire (per weight percentage).

Fe	C	Mn	Si	P	S
Balance	0.05	1.4	0.5	0.02	0.02

Table 3. Chemical composition of electrode E7018 [manufactured by Ama Company] (per weight percentage).

Fe	C	Mn	Si	S	P
Balance	0.06	1.5	0.3	0.02	0.02

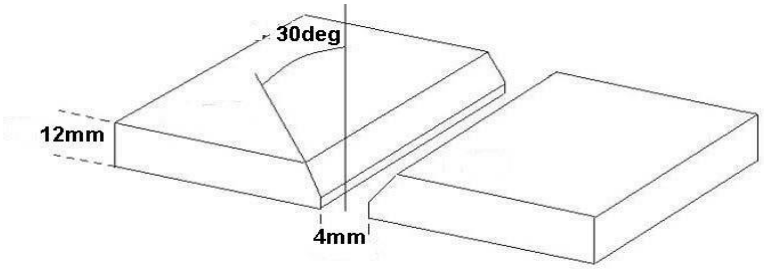

Fig. 1. Joints scheme utilized in welding samples.

Table 4. FCAW parameters exercised for ST-37.

Filler diameter	polarity	velocity (mm/s)	Voltage (V)	current (A)	protective gas
1.2	DCRP	1	32-21	300-200	CO_2

Table 5. SMAW parameters exercised for ST-37.

parameters	value
Electrode class	E7018
Number of passes	three passes
Welding condition	3G
Electrode diameter (mm)	3.2
current intensity (A)	95-120
polarity	DCRP
Voltage (V)	18-28
Welding speed (cm/min)	6-10
Maximum input heat (kJ/mm)	2

A tensile test was performed at room temperature to compare the yield and tensile strength changes of welded samples. A weld transverse tension test was conducted in a manner consistent with American Society of Mechanical Engineers (ASME) standards by the GOTECH AL-7000-LA60 machine. Fig. 2. presents two transverse tensile weld samples consistent with ASME standards. Consistent with the ASME standard, the transverse tensile strength of the weld should not be lower than the minimum tensile strength determined for the base metal [14].

Hardness changes in different parts of the ST-37 steel weld joint were measured consistent with the standard (ISO 6507-1:2005) by a Vickers hardness tester with a force of HV5 (49.03N). Fig. 3. shows the schematic of the joint plan and hardness measurement points.

Moreover, the Charpy impact test was performed according to the ASTM E23 standard by the SANTAM at room temperature on the weld metal. Fig. 4. displays the schematic of the joint design and the position of the impact samples whose gap is located in the base metal and weld zone. Fig. 5. shows the dimensions of the Charpy impact samples. Additionally, three Charpy impact tests were performed for each sample, and the average energy absorbed in the three tests was determined. Following the fracture cross-sectional test, the samples were tested using the TE-SCAN MIRA3 scanning electron microscope.

3. Results and Discussion

3.1. Transverse Tensile Test

A transverse tensile test of the ST-37 steel weld joint was performed to determine the appropriate welding technique in terms of the desired welding properties for the joint. Tables 6 and 7. present the results of the transverse tension tests for the FCAW and SMAW, respectively.

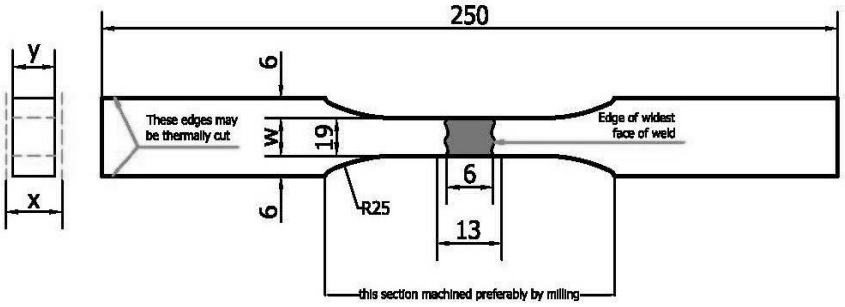

Fig. 2. Dimensions of tensile welding samples [14].

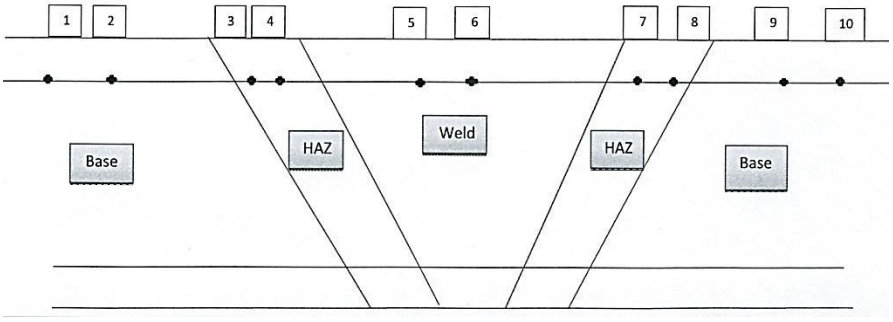

Fig. 3. Schematic of the joint plan and hardness measurement points.

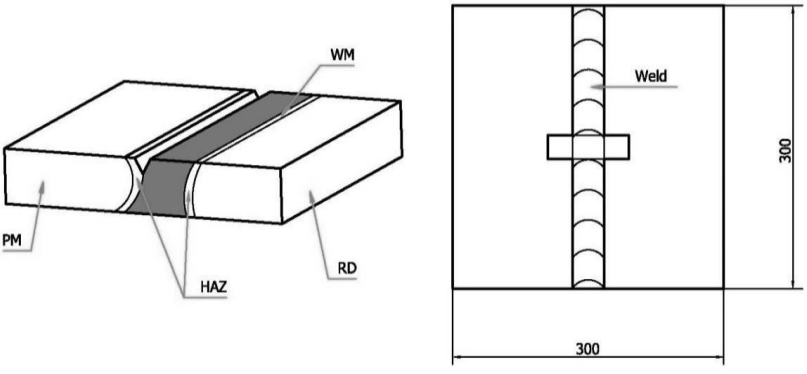

Fig. 4. Schematic of joint design and position of impact samples [15].

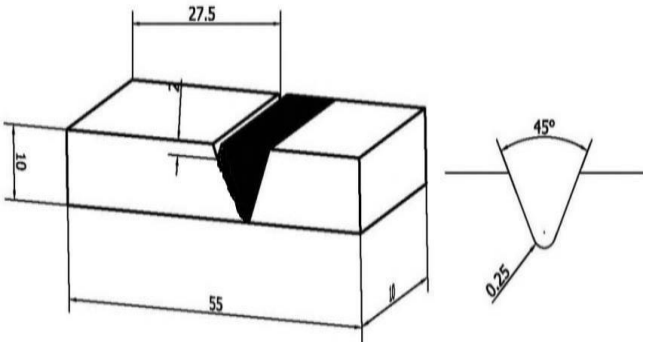

Fig. 5. Dimensions of the tested impact samples [15].

Table 6. Tensile test results for FCAW.

Width (mm)	Thickness (mm)	Area (mm^2)	Ultimate strength (N/mm^2)	failure zone	Tensile test sample
19.08	7.89	150.54	414	Base Metal	T1
19.13	7.7	147.3	419	Base Metal	T2

Table 7. Tensile test results for SMAW.

Width (mm)	Thickness (mm)	Area (mm^2)	Ultimate strength (N/mm^2)	failure zone	Tensile test sample
19	8.01	152.19	418	Base Metal	T1
19.12	8	152.96	405	Base Metal	T2

Fig. 6. compares tensile test results of transverse tensile weld samples of the two welding techniques. Consistent with ASME IX [14], the transverse tensile strength must not be less than the minimum tensile strength determined for the base metal. However, the results show that the strength of the resulting weld is higher than that of the ST-37 base metal, and the tensile sample is broken from the ST-37 base metal. Furthermore, the failure of the transverse tensile weld sample from the base metal shows no defects affecting the weld properties in the sample. Accordingly, the quality of the weld was confirmed. Fig. 6. displays the comparison of both joints. As the Figure displays, the values in the sample welded with FCAW are more than those with SMAW.

Considering that the ST-37 utilized in the construction of steel structures has a yield stress equal to 240 MPa and for sheets whose yield stress is up to 300 MPa and thickness equal to or less than 15 mm, E60 and E70 electrodes are likely to be applied. Moreover, a 12 mm thick steel sheet and E70 electrode are applied to the paper. Since the 10th topic of Iran's National Construction Regulations is derived from AISC 360, for sheets with a thickness equal to or less than 15 mm and yield stress of up to 300 MPa and using an E70 electrode or equivalent, the final tensile strength of the weld must be higher than 420 MPa [16, 17]. Considering that the transverse tensile samples of both connections are broken at the base metal, the weld strength is more than 420 MPa, according to the requirements of this regulation, and the weld strength is approved. Fig. 7. shows the fracture location of tensile samples. Moreover, the results of transverse welding tensile tests show that welding of ST-37 steel joints is likely to be performed using both techniques.

3.2. Hardness measurement results

FCAW with E71T filler metal and SMAW with E7018 electrode were applied to measure hardness.

Tables 8 and 9. present the results of both welding techniques' Vickers hardness measurement. Moreover, to determine the hardness changes, the hardness profile of weld metal, HAZ, and ST-37 base metal was consistent with Fig. 8.

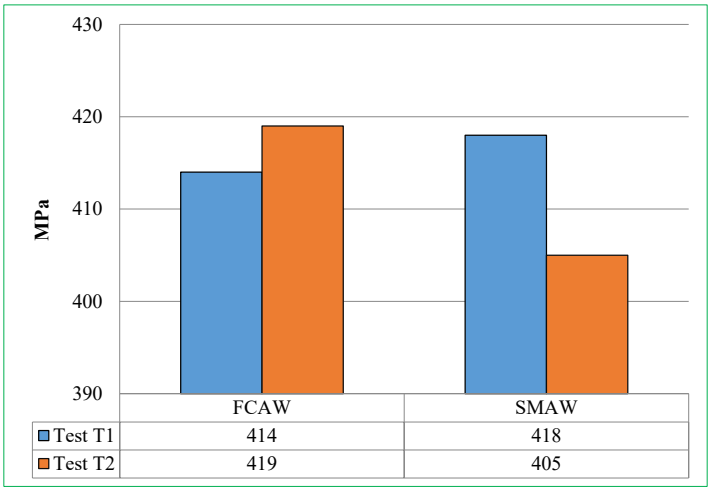

Fig. 6. Comparison of ultimate strength of FCAW and SMAW joints.

Fig. 7. The fracture zone of the two tensile samples.

Table 8. Hardness measurement results of ST-37 steel welding by FCAW and SMAW technique.

Vickers hardness (HV)		Hardness measurement position
Welding sample FCAW	Welding sample SMAW	
134	135	Base
135	136	Base
148	159	HAZ
149	160	HAZ
185	206	Weld
183	209	Weld
143	152	HAZ
142	151	HAZ
136	136	Base
133	134	Base

Table 9. Average welding hardness of ST-37 steel by FCAW and SMAW technique.

Average hardness of the base metal(HV)	Average difficulty HAZ (HV)	Average weld hardness (HV)	sample
135	155.5	207.5	Welding sample SMAW
134.5	145.5	184	Welding sample FCAW

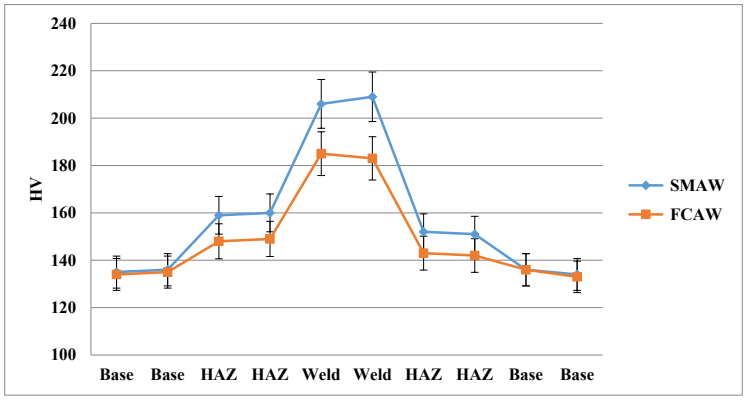

Fig. 8. Changes in Vickers hardness of ST-37 steel weld joint by FCAW and SMAW technique.

The results show the hardness of the heat-affected zone on both sides of the ST-37 steel joint. Furthermore, the hardness of the zone decreases with the increase of the input heat of welding because of the higher input heat of FCAW compared to SMAW. Accordingly, the SMAW welding sample has the lowest heat input and the highest hardness in the heat-affected zones, and the FCAW sample has the highest heat input and the lowest hardness in the heat-affected zones.

The average hardness value in different welding zones of the FCAW and SMAW samples exhibits the hardness variation across the welding zones in two samples with varying welding techniques, indicating the dominant inhomogeneous structure in different welding zones.

Moreover, the average values of Vickers hardness for the base metal and HAZ additionally show that the same behavior as the weld metal is the same in the two samples. The average value of HAZ hardness on both sides of the weld joint was higher than that of the base metal. The SMAW sample, however, had the highest HAZ hardness compared to the FCAW sample. The lower hardness of the heat-affected zone in the FCAW sample was because of the increase of the welding input heat due to the welding operation on both sides of the samples.

Techniques with high heat input are usually operated for high-strength steel welding, such as FCAW. However, these welding methods reduce the cooling rate of the heat-affected areas of the HAZ and cause grain growth in the steel structure, leading to the worsening of the HAZ characteristics, including its hardness [18, 19].

The effects of the welding input heat on the microstructure and mechanical properties of the HAZ zone in high-strength, low-alloy steel joints are well studied, and the results show that Vickers hardness in HAZ and FZ zones in steel joints is much higher than base metal. However, the average hardness of HAZ decreases with the increase of welding input heat [20].

As Table 9. exhibits, the weld metal in the SMAW sample has the highest hardness, and the FCAW sample has the lowest hardness of the weld metal; because of the increase in the input welding heat, the hardness of the E71T weld metal decreases, which attribute to the change in the morphology of the weld metal structure due to the application of heat input during welding. As the input heat increases, the cooling rate decreases, making it possible for the weld to remain in higher temperature ranges for longer. Furthermore, coarse grains produced will result in a decrease in hardness [21].

3.3. Charpy impact test results

The impact test was performed on ST-37 base metal, E71T weld metal of FCAW, and E7018 weld metal of SMAW at room temperature. Table 10. presents the impact test results of the sample welded by FCAW and SMAW techniques. As Table 10. and Fig. 9. show, however, E71T weld metal samples of FCAW have lower impact energy than the E7018 weld sample of SMAW. This reduction in weld metal impact energy in the connection of ST-37 steel using E71T filler metal is likely to be caused by the higher welding input heat and the inhomogeneous structure of the weld metal, which may additionally be observed in the hardness of the E71T weld metal.

Table 10. The results of the impact test of samples at room temperature.

Average impact energy (J)	Impact energy (J)	The place of the gap	Sample
81	91	Weld	Welding sample FCAW
	69		
	83		
86	92	Weld	Welding sample SMAW
	93		
	75		

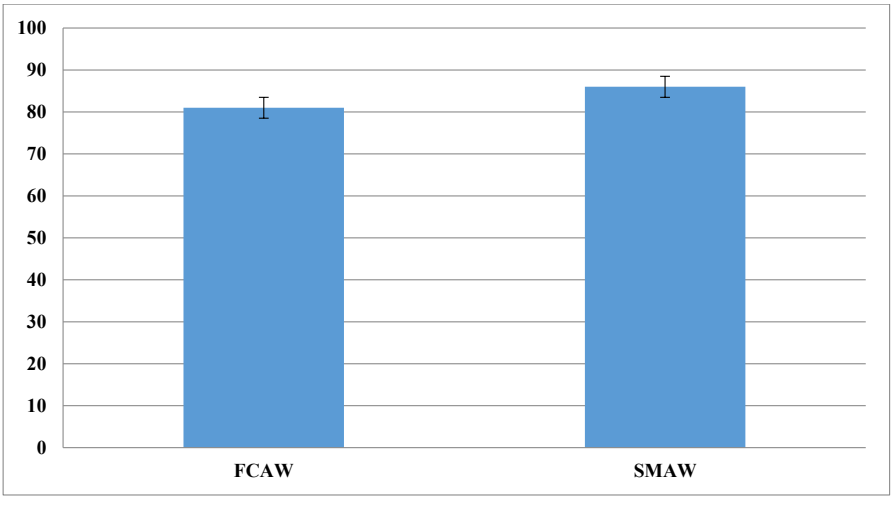

Fig. 9. Bar graph of the average energy of FSAW and SMAW.

In the seismic regulations of the 10th topic of Iran's National Building Regulations and AISC 341-10 regulations, the welds used in connections are divided into two categories: first, the welds used in the connections and patches of the members of the seismic lateral load-bearing system, as well as the patch of non-load-bearing columns; and second, is the "critical requirement " welds, such as groove welds with full penetration in unique and medium bending frames and beam connections of divergent braced frames [17, 22]. For Category II welds in the AISC Code, the strength of a given Charpy groove specimen of the weld metal at 20°C shall be at least 54 J. Therefore, considering that the average Charpy impact test of three samples of both welding joints is more than 54 joules [22] in the sheet thickness of 12 mm, it meets the seismic requirements for welding.

As Table 10. and Fig. 9. show, the impact toughness of the weld metal in the FCAW weld sample is lower than that of the SMAW weld metal, as the input heat increases because of grain coarsening and additionally the inhomogeneity of the steel structure, the fracture energy decreases. As the grains grow, the crack may propagate along more accessible paths between the grains. Increasing the input heat also increases the percentage of sediments that are likely to be the source of cracks, and as a result, they reduce the fracture energy. However, coarse structure is one of the main factors of toughness deterioration. Typically, the coarse structure leads to a decrease in the toughness of the HAZ and the weld metal. The compounds in the structure play an essential role in the toughness or brittleness of HAZ and weld metal [18, 19].

A scanning electron microscope studied the fracture cross-section of the impact weld samples in the connection of ST-37 using FCAW and SMAW techniques. Figs. 10 and 11. present the fracture surfaces electron microscope images of weld metal of FCAW and SMAW samples. The morphologies of the fracture surfaces identified in the fracture observations include soft and brittle dimples. Moreover, the morphology of soft dimples represents the fracture mechanism of the connection of cavities. It indicates the occurrence of soft or ductile fracture through the germination and joining of cavities [23, 24].

As Fig. 10. shows, under these conditions, the fracture surface shows a dimple morphology in the E71T filler metal sample of FCAW (Fig. 11a). Also, holes and dimples are visible in the structure (Fig. 11b). Points A, B, and C are the sediments in the structure contain aluminum, silicon, oxygen, titanium, manganese, and sulfur elements in the EDS spectrum. As evidenced in the EDS spectrum of these deposits at Points A, B, and C,

(Figs. 10 c, 10 d, and 10 e, respectively) the presence of oxygen, aluminum, and titanium elements is confirmed with a very high percentage compared to other elements, which indicates that these deposits are compounds of titanium aluminide and aluminum and titanium oxides. Furthermore, aluminum and titanium elements may be present in the chemical composition of the E71T filler metal, which has caused the formation of intermetallic compounds in the weld metal. These deposits may weaken the impact resistance of the E71T weld metal.

Fig. 11. shows the fracture surfaces of the weld metal. The change of fracture mechanism or the creation of a crack growth path along the grain boundaries is not observed. The fracture surface shows a dimple morphology in the E7018 electrode sample of SMAW (Fig. 11b). However, the presence of dimples and holes is observable in the structure. Large dimples on the fracture surface indicate a completely soft fracture (Fig. 11c). The origin of these holes in the structure may be attributed to the sediments. Points A (Fig. 11e) and B (Fig. 11f) in the EDS spectrum of sediments contain elements of titanium, manganese, and silicon.

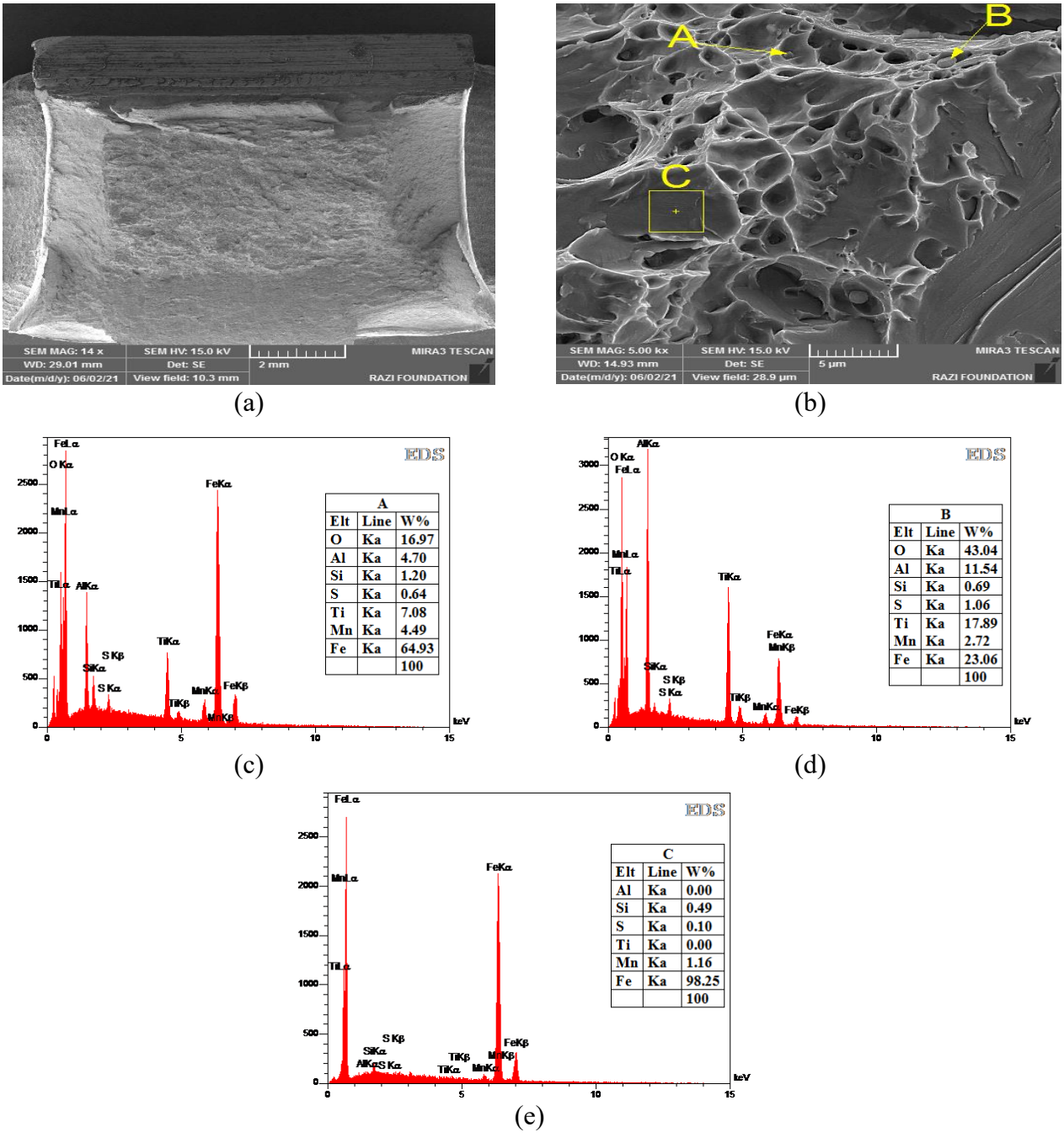

Fig. 10. SEM images with (a) dimple morphology of the fracture surface (b) place of deposition of points and EDS spectra at points A (c), B (d), and C (e) of the fracture section of the FCAW weld metal impact sample.

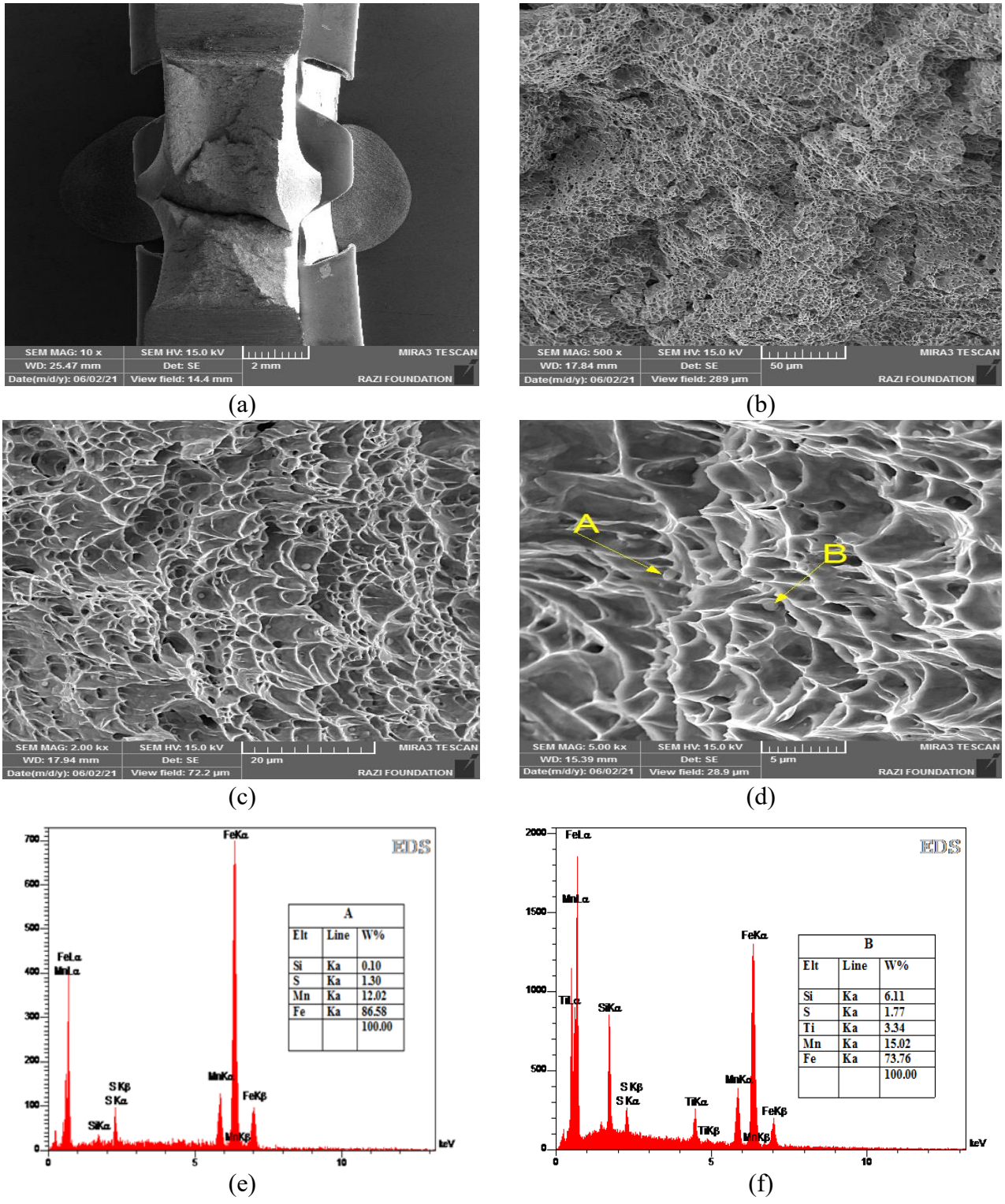

Fig. 11. SEM images with (a) dimple morphology of the fracture surface, (b) holes and dimples in the structure, (c) holes and dimples in a closer view, (d) place of deposition of points and EDS spectra at points A (e) and B (f) of the fracture section of the E7018 electrode impact sample of SMAW.

4. Conclusions

The paper studies two samples of ST-37, which were joined using E71T-1C filler metal by FCAW and E7018 electrode by SMAW. Moreover, tensile strength, hardness, and weld impact resistance were studied.

Accordingly, the following conclusions are drawn:

- The tensile test results of both samples welded with E71T-1C filler metal of FCAW and E7018 electrode of SMAW method showed that the strength of the resulting weld is higher than the base metal so that therefore the tensile sample failed at the location of ST-37 base metal. Additionally, the final tensile strength of the FCAW welded sample was higher than that of the SMAW welded sample.
- The filler metal E71T of FCAW meets the requirements of the weld's final strength based on the AISC 360 regulation's seismic criteria and the 10th topic of the National Building Regulations of Iran.
- Furthermore, the hardness of the heat-affected zone increased compared to ST-37 steel in both welding techniques, and with the increase of welding heat input, the HAZ hardness decreased. The average weld metal hardness for SMAW and FCAW was 207 and 184 Vickers, respectively.
- The average impact energy of SMAW weld metal (86 J) is higher than that of the FCAW (81 J) sample. However, the lower impact energy of FCAW metal decreases because of higher input heat and the coarsening of the weld fracture energy structure.
- The E71T filler metal for FCAW provides the required impact resistance at a temperature of 20°C. Therefore, the technique is applicable for joint groove welds based on the seismic criteria of the 10th topic of Iran's National Building Regulations and the AISC 341-10.

References

[1] Mehrabi Gohari E, Mohammadi M, Nozari M, Bagherpour H, Thermal analysis of laser welding in joint of stainless steel to low carbon steel using finite element method (FEM), Modares Mech Eng. 2019; 19(6): 1475–82.

[2] Ion J, Easterling K.E, Computer modeling of weld-implant testing. Mater Sci Technol. 1985; 1(5): 405–11.

[3] Taylor D, Barrett N, Luciano G, Some new methods for predicting fatigue in welded joints, Int J Fatigue. 2002; 24(5): 509–18.

[4] Yakubovski V, Valteris I, Geometrical parameters of butt and fillet welds and their influence on the welded joint fatigue life. IIW Doc. 1989; 13: 1326-89.

[5] AWS. Materials Welding Handbook, Volume 1 – Welding Technology. American Welding Society; 2000.

[6] Zohrehvand A, Farahani M, Cladding of carbon steel with aluminum stainless layer using friction stir welding method, Modares Mech Eng. 2017; 17(4): 410–8.

[7] Babu S, David S, Quintana M, Modeling microstructure development in self-shielded flux cored arc welds, Weld J N Y. 2001; 80(4): 91S–97S.

[8] Gadallah R, et al. Influence of shielding gas composition on the properties of flux-cored arc welds of plain carbon steel, Int J Eng Technol Innov. 2012; 2(1): 1.

[9] Xu C, et al. Influence of welding speed on weld pool dynamics and welding quality in underwater wet FCAW, J Manuf Process. 2020; 55: 381–8.

[10] Sahali M.A, Multi-objective optimization of FCA welding process: trade-off between welding cost and penetration under hardness limitation, Int J Adv Manuf Technol. 2020; 110(3): 729–40.

[11] Awali J, et al. Analisis variasi arus pengelasan kombinasi SMAW-FCAW dengan kampuh double V-groove terhadap kekerasan dan struktur mikro dissimilar material JIS G3101-SS400 dan ASTM A36, J Rekayasa Mesin. 2021; 12(2) :421–32.

[12] Maijuansyah M, et al. Study on the thermal distortion, hardness, and microstructure of St 37 steel plate joined using FCAW, J Mech Eng Sci Technol. 2019; 3(1): 18–28.

[13] Jannifar A, et al. Welding current effect of welded joints of base metal St37 on characteristics: corrosion rate and hardness. In: IOP Conference Series: Earth and Environmental Science, IOP Publishing; 2019.

[14] Yuan C.L, Yu C.L, Microstructure and tribological performance of Ti-6Al-4V cladding with SiC powder, Surf Coat Technol. 2011; 205: 5400–5.

[15] de Albuquerque V.H, de Macedo Silva E, Leite J.P, de Moura E.P, de Araújo Freitas V.L, Tavares JM. Spinodal decomposition mechanism study on the duplex stainless steel UNS S31803 using ultrasonic speed measurements, Mater Des. 2010; 31(4): 2147–50.

[16] American Institute of Steel Construction. Specification for Structural Steel Buildings. Chicago: American Institute of Steel Construction; 2010. (AISC-10-360).

[17] National Building Regulations of Iran, Tenth Theme, Designing and Implementing Steel Buildings. Engineering Bureau Office; 1392. Third Edition.

[18] Wan X.L, Wu K.M, Huang G, Wei R, In situ observations of the formation of fine-grained mixed microstructures of acicular ferrite and bainite in the simulated coarse-grained heated-affected zone, Steel Res Int. 2014; 85(2): 243.

[19] Wan X.L, Wei R, Wu K.M, Effect of acicular ferrite formation on grain refinement in the coarse-grained region of heat-affected zone, Mater Charact. 2010; 61: 726.

[20] Dong H, Hao X, Deng D, Effect of welding heat input on microstructure and mechanical properties of HSLA steel joint, Metallogr Microstruct Anal. 2014; 3(2): 138–46.

[21] Lundin C.D, Zhou G, Khan K.K, Report Number 1: Metallurgical characterization of the HAZ in A516-70 and evaluation of fracture toughness specimens. Bull Weld Res Counc. 1995 ; 1(403).

[22] American Institute of Steel Construction. Seismic provisions for structural steel buildings. Chicago: American Institute of Steel Construction; 2002.

[23] Mills W.J, Fracture toughness of type 304 and 316 stainless steels and their welds, Int Mater Rev. 1997; 42(4): 45–82.
[24] Beyhaghi M, Investigation of influences of mechanical activation and heating rate on nanostructured NiAl-Al_2O_3 composites formation by combustion synthesis, Adv Process Mater Eng. 2017; 11(2): 1–25.